Renewable and Sustainable Energy Reviews 16 (2012) 1709–1720

Contents lists available at SciVerse ScienceDirect

Renewable and Sustainable Energy Reviews

journal homepage: www.elsevier.com/locate/rser

Characterization of solar flat plate collectors

F. Cruz-Peragon [a], J.M. Palomar [a], P.J. Casanova [b], M.P. Dorado [c], F. Manzano-Agugliaro [d,*]

[a] Dept. of Mechanics and Mining Engineering, EPS de Jaen, Universidad de Jaen, Campus Las Lagunillas s/n, 23071 Jaen, Spain
[b] Dept. of Electronics Engineering and Automation, ESP de Jaen, Universidad de Jaen, Campus Las Lagunillas s/n, 23071 Jaen, Spain
[c] Dept. of Physical Chemistry and Applied Thermodynamics, EPS, Campus de Rabanales, Universidad de Cordoba, Campus de Excelencia Internacional Agroalimentario, ceiA3, 14071 Cordoba, Spain
[d] Dept. Rural Engineering, University of Almería, 04120 Almería, Spain

ARTICLE INFO

Article history:
Received 8 March 2011
Received in revised form
21 November 2011
Accepted 25 November 2011
Available online 18 January 2012

Keywords:
Model optimization
Numerical approach
Solar collector
Correlation functions

ABSTRACT

Characterization of solar collectors is based on experimental techniques next to validation of associated models. Both techniques may be adopted assuming different complexities. In this work, a general methodology to validate a collector model, with undetermined associated complexity, is presented. It serves to characterize the device by means of critical coefficients, such as the film (convection) transfer coefficient, plate absortance or emmitance. The first step consists of identifying those significant parameters that match the selected model with the experimental data, via nonlinear optimization techniques, applied to steady state conditions. Second, new correlations must be adopted, in those terms where it is necessary (i.e. film coefficient equations). Finally, the overall model must be checked in transient regime. To illustrate the technique, a tailor-made prototype flat plate solar collector has been analyzed. An intermediate complex collector model has been proposed (2D finite-difference method). Both steady and transient states were analyzed under different operating conditions. Parameter identification is based on Newton's method optimization. For parameter approximation, exponential regression functions through multivariate analysis of variance is proposed among many other alternatives. Results depicted a robustness of the overall proposed method as starting point to optimize models applied to solar collectors.

Contents

1. Introduction and previous work

Processes of industrialization and economic development require important energy inputs [1]. Fuels are the world's main energy resource and are considered the center of energy demands. However, reserves of fossil fuels are limited and their large-scale use is associated with environmental deterioration [2]. These facts

Abbreviations: CFD, computational fluid dynamics; FEM, finite element method; IHTP, inverse heat transfer problem; RMSE, root mean square error.

* Corresponding author. Tel.: +34 950015396; fax: +34 950015491.
E-mail addresses: fcruz@ujaen.es (F. Cruz-Peragon), jpalomar@ujaen.es (J.M. Palomar), casanova@ujaen.es (P.J. Casanova), pilar.dorado@uco.es (M.P. Dorado), fmanzano@ual.es (F. Manzano-Agugliaro).

1364-0321/$ – see front matter © 2011 Elsevier Ltd. All rights reserved.
doi:10.1016/j.rser.2011.11.025

Nomenclature

a_l	constant factor of the regression function 'l'
b_{ul}	exponent (constant value) of the regression function 'l'
Bi	Biot number
c_f	fluid specific heat (J/(kg K))
c_p	specific heat of the absorber plate (J/(kg K))
D_i	inner diameter of the risers (m)
e	plate thickness (m)
e_q	2D equivalent thickness of the pipe-weld-plate (m)
e_r	pipe thickness (m)
f_l	exponential regression function 'l'
Gr	Grashof number
h	final estimated film coefficient of the inner wall water (W/(m^2 K))
h_o	initial film coefficient of the inner wall-water (W/(m^2 K))
I_T	global incident radiation over tilted surface (W/m^2)
k_e	extinction coefficient of the covering glass (m^{-1})
k_f	pipe conductance (W/(m K))
k_p	conductance of the absorber material (W/(m K))
k_h	proportionality factor applied to h
k_q	proportionality parameter associated to the volumetric equivalent heat transfer coefficient U_c
k_{uc}	proportionality factor applied to U_c
k_{iT}	conduction heat transfer coefficient of the insulation material (W/(m K))
K_c	global heat transmission coefficient plate-fluid (W/(m^2 K))
$\dot{m}_f$	fluid flow rate into the risers (kg/s)
$\dot{m}'_f$	fluid flow rate in lower and upper pipes (kg/s)
n_2	refraction index of the covering glass
Nu	Nusselt number
Pr	Prandtl number
q''_1	unitary surface heat radiation on the absorber (W/m^2)
$\dot{q}_1$, S	internal heat generation in the absorber due to solar radiation (W/m^3)
q''_2	unitary surface heat loss in the absorber plate (W/m^2)
$\dot{q}_2$	loss of the internal heat generation in the absorber (W/m^3)
q''_3	unitary surface heat transferred to the working fluid (W/m^2)
$\dot{q}_3$	loss of the internal heat generation in the absorber due to heat transmission to water (W/m^3)
$\dot{q}_v$	internal heat generation in the absorber (W/m^3)
q'_u	net heat released in the refrigerant water per length unit (W/m)
r_i	inner radius of the riser (m)
r_e	outer radius of the riser (m)
r'_i	inner radius of lower and upper pipe (m)
Re	Reynolds number
s	collector tilt (rad)
$\overline{SP}^n$	known conditions vector at time 'n'
t	time (s)
T	temperature (K)
T_a	cuidado si es T_o (Eq. (2.b))
T_o	room temperature (K)
T_b	plate temperature in the bulb thermometer (K)
T_{fi}	refrigerant fluid inlet temperature (K)
T_{fo}	refrigerant fluid outlet temperature (K)
T_f	fluid mean temperature in a differential element (K)
$T_{f,p}$	fluid temperature into the upper and lower horizontal pipes(K)
T_p	material temperature of the upper and lower horizontal pipes (K)
T_m	mean top surface temperature (K)
T_w	mean temperature in the inner side of the pipe in a differential element (K)
$\overline{UP}^n$	Unknown parameters vector at a stationary state at time 'n'
U_L	volumetric heat transfer loss coefficient of the collector (W/(m^3 K))
U_l	global heat loss coefficient of the collector (W/(m^2 K))
U_b	heat loss behind the collector (W/(m^2 K))
U_t	top heat loss (W/(m^2 K))
U_C	volumetric equivalent heat transfer coefficient of the control volume pipe-weld-plate (W/(m^3 K))
X_{ul}	standardized input parameter 'u' of a regression function for output parameter 'l'
x	transversal direction distance in the collector (m)
y	longitudinal direction distance in the collector (m)
α	thermal diffusivity of the absorber plate material (copper) (m^2/s)
α_θ	directional absorbance of the cooper black plate
Δ	increment
ε_g	glass emmitance
ε_p	plate emmitance
ρ	absorber density (kg/m^3)
ρ_f	refrigerant density (kg/m^3)
φ	latitude (rad)
ω	timing angle (rad)
δ	declination (rad)
γ	azimutal angle (rad)
θ	incident angle of beam irradiance over the tilted surface (rad)
Ψ	objective function to minimize by the identification process
Γ	auxiliary expressions for Eqs. (7.a), (7.b), (9.a) and (9.b)

Sub-index

i	x direction
j	y direction
m	number of nodes in x direction
w	number of input parameters in a regression function
p	number of riser
r	node number

Super-index

k	time in transient regime analysis
n	interval of time

have encouraged growth in the use of renewable energy resources worldwide [3]. Solar energy is considered one of the main promising alternative sources of energy to replace the dependency on other fossil energy resources [4,5]. Solar water heating systems are very common systems, extensively used in many countries with high solar radiation potential, such as Mediterranean countries [6]. They are often viable to replace fossil fuels used for many home applications [7]. Conventional flat plate solar collectors with a metal absorber plate and covers are used to transform solar energy into heat [8]. Optimization of solar heating systems provides both running and design parameters that ensure maximal collected heat.

Main parameters to be considered are related with both geometry and materials properties [9–16]. An optimal design must ensure minimal working fluid pressure loss, besides a nearly constant temperature on each transversal section of the plate. Otherwise, temperature between pipes will rise, thus increasing radiation heat loss. To carry out the optimization of the process, a system simulation, including model validation and analysis under different working conditions are needed. In this sense, the first step consists of determining the parameters associated to heat collection and transmission. Subsequently, a mathematical model considering the following premises must be established:

a) *Parameters associated to the physical properties of the system*. According to the literature, main material properties that influence the system are well known [17–19]. Conventional absorber plates usually exhibit either parallel or serial hydraulic configurations. These configurations (including "Z" configuration) besides circulating regimes showing small Reynolds number (*Re*) lead to non-uniform flow distribution. On the other hand, heat transfer from wall to working fluid leads to non-uniform transversal temperature distribution on the plate. Thus, disregard of some critical parameters related to both fluid flow and heat transfer by convection makes difficult the optimal design of the system. Although primary surface pressure loss can be easily estimated [20,21], little research about coefficients of pressure loss in junctions and bifurcations in collector pipes has been done. In fact, previous works only consider parameters dependent on *Re* at different flow ratios [22,23]. Flow ratio is defined as the relation between the discharge in each riser (being riser no. 1 the nearest to the inlet port) and the total discharge of the collector. In this sense, there is an extensive literature devoted to semi-empirical correlations for film coefficients approximation [24–26]; however, correlations for pressure loss in junctions and bifurcations are still needed [27,28]. On the other hand, extremely small *Re* means axial flow velocity is distorted. This feature makes difficult to understand and approximate the process [29]. Also, flow distribution seems to be strongly influenced by the Grashof number (*Gr*) and the pipe leans [30,31].
b) *Simulation complexity*. Collector characteristics are usually well known and needed for model design. However, system characterization may increase the complexity of the model. This complexity can be described under both stationary and transient regimes through computational fluid dynamics (CFD) methods [19,32–35]. The target is to reach a compromise between the complexity of the selected model and the accuracy of its results, which should adequately simulate the system behavior.

Single-dimensional methods are able to simulate with high accuracy the majority of the situations. Nevertheless, to carry out an optimal design, two-dimensional methods based on finite difference or control volume techniques must be considered, so a good fitting can be achieved [36,37]. In this sense, to determine the temperature distribution over the plate, an adequate simulation of the heating system entails an associated mathematical difficulty, considering both characterization and CFD techniques. In fact, in case experimental data show high temperature difference between upper tubes, previous models are useless [36,38,39].

For these reasons, validation of a defined numerical or mathematical model involves data acquisition and identification of parameters that show abnormal behavior according to the literature. Eventually, it can force to re-define some of the equations associated to the model.

Thus, the objective of this work is to propose a complete procedure to optimize the equations associated to a collector model. In the first step, the identification of the parameters associated to materials and heat transfer provides the system validation over the time. Then, previous values will help to provide new correlation functions associated to the collector behavior. In sum, a first approach to optimize a two-dimensional finite difference model associated to a flat plate solar collector with low flow rate is proposed.

Identification of a thermo-physical process involves the determination of its parameters by solving an inverse heat transfer problem (IHTP). Inverse problems consist in the determination of the initial parameters when solutions are known. This kind of analysis has been proposed by many researchers during the past years [40,41]. Also, it has been proved that solutions to IHTP are usually unique, though estimations are not always numerically stable [42]. In this work, an inverse problem (identification procedure) is performed by means of iterations over a direct problem (system model) using a derivative dependent method. The identification is based on a non-linear optimization technique that uses an objective function, Ψ, obtained from the sum of squares of the differences between the model and the experimental values [43,44]. This quadratic form provides the best performance in a wide range of engineering optimization problems. This technique applies the second order Newton minimization method, in combination with a Taylor expansion series of Ψ, truncated to the third derivative [43]. According to the literature, it is observed that the solution set (temperatures) is continuous and smooth, without drastic changes [36,38,39]. The same assumptions have been applied to heat transfer problems [45]. For these reasons, when a quasi-Newton method truncated to the second derivative is selected, the computational efforts are reduced while keeping their accuracy [43]. If the number of measured points (in terms of time-space) is not lesser than the number of parameters to be identified, the solution of a non-linear steady IHTP is unique. The simultaneous identification of thermo-physical characteristics, internal heat source and heat flux would be unique if either before or during the numerical experiment, the monotonicity or piecewise-monotonicity of the parameters to be determined is found to be likewise [40]. In the present work, none of these premises fulfil the problem conditions because only two sensors were used. For this reason, results only describe a general approach. Nevertheless, specificity could be increased by adding more sensors over the absorber and into the risers.

2. Materials and methods

2.1. Equipment

The solar collector system, as shown in Fig. 1, is composed of a set of parallel copper pipes under a 'Z' disposition. They are attached to a copper flat plate (absorber) by means of a tin–silver (6%) welding. This assembly is covered with a matt black paint coating, operating as a selective surface, thus making possible a great radiation collection. The casing is made of a white-lacquered aluminium profile. Two frames of this type are superposed. One of them contains white glass, while the other one contains the pipes-plate unit. The isolator is composed of two thin aluminium sheets separated by an expanded polystyrene layer. It incorporates inlet and outlet water thermometers and manometers, next to a bulb thermometer placed on the absorber plate. Security valves are attached to this equipment. The main characteristics and material properties of this collector are shown in Table 1. They provide an accurate simulation of the system [46].

2.2. Collector model

Analyses must be carried out under rigorous model conditions, including the main features of a representative dynamic

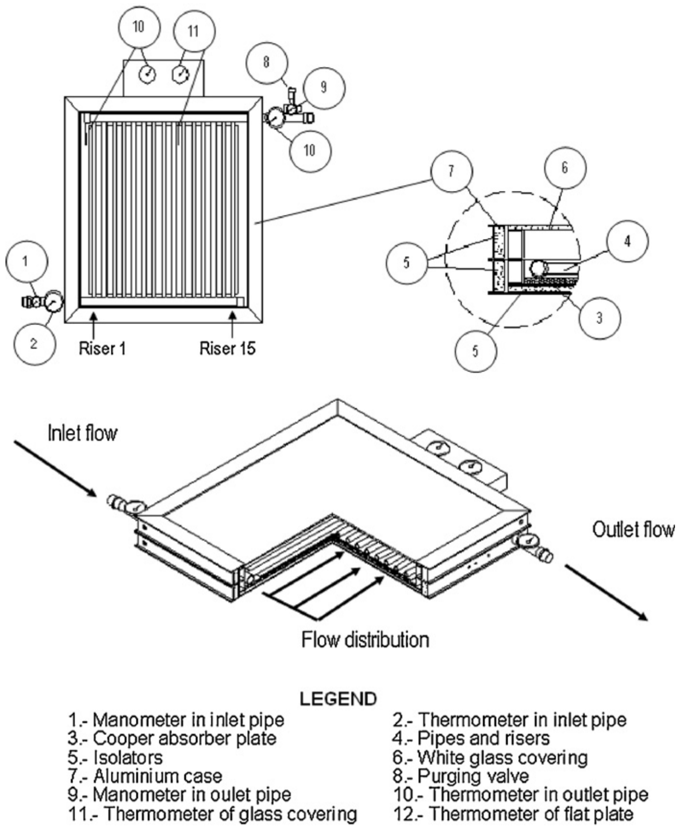


Fig. 1. Collector under study.

Table 1
Collector properties.

Property	Value
Absorber material	Copper
Absorber thickness (mm)	2
Absorber useful surface (m^2)	0.21
Inner diameter of the horizontal tubes, R'_T (mm)	20
Inner diameter of the riser, R_i (mm)	10
Number of risers	15
Riser length (mm)	450
Distance between risers (mm)	30
Glazing thickness (mm)	4
Complete useful surface (m^2)	0.37
Posterior insulation (mm)	10 (aluminium sandwich) + 7 (polyurethane)
Collector plate efficiency factor, F_R	0.7

simulation model and applied only to the plate-risers unit [47]. In this particular case, the following conditions were adopted:

(i) A heat transfer analysis by finite difference approach of the absorber plate and the fluid that flows through the pipes must be carried out. Some simplifications consider the plate as a two-dimension system and each pipe as a one-dimension system. The model consists of a set of non linear equations for both steady and transient states, which must be solved by iterations [48].

(ii) Conduction coefficients and diffusivities of the plate, pipes and cover, as well as insulating materials must be taken into consideration. On the other hand, densities, specific heat, viscosity, conductivity and Prandtl number of the circulating fluid (water) are approximated by 4th-order polynomial functions, depending on the fluid temperature [49]. The necessary data are collected from the literature [50].

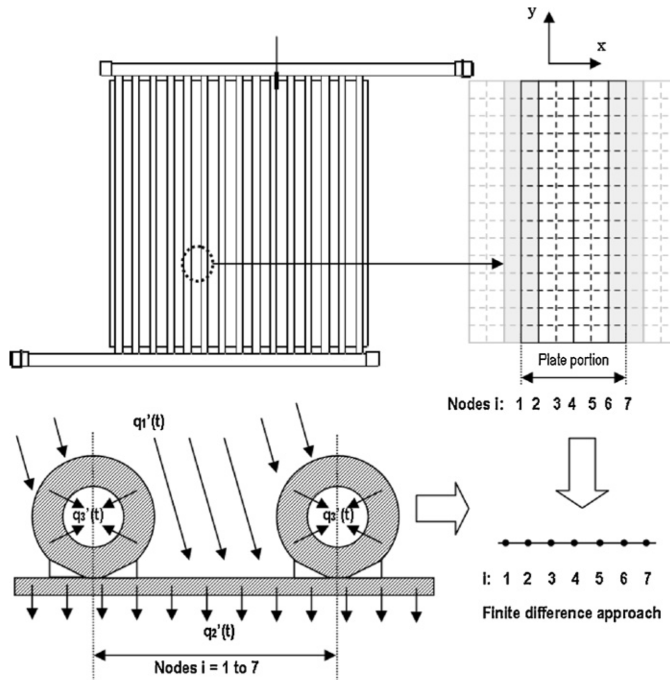


Fig. 2. Sample network.

(iii) Heat loss coefficients of the plate are considered to be dependent on both average and room temperatures, at each interval of time.

(iv) Temporary variations of irradiation, room and water inlet temperatures are considered model inputs. In this sense, both the unitary heat release of the tilted surface (adjusted with the help of an isotropic model, with reflectance equal to 0.2) and the absorptance–transmittance product depend on time [17]. Additionally, time variations of water outlet temperature and bulb temperature (over the flat plate) are known but only used during the identification process.

(v) According to Streeter et al., flow distribution into each pipe may be calculated by means of the friction loss and conventional techniques [20]. However, secondary loss coefficients applied to collector junctions and bifurcations are both *Re* (of the main pipe flow) and flow rate dependent [22]. According to Wietbrecht et al., they may be approximated by exponential functions [22].

(vi) Film heat transfer coefficients are initially approached by means of semi-empirical equations [24,25,28,50,51]. Although there are many particular correlations, those listed in Incropera et al. have been selected [50]. Once the optimization process is finished, the coefficients are empirically evaluated to validate the model.

To carry out the analysis, the absorber surface was divided into multiple similar units, using a mesh, so it could be considered a discrete problem. A grid sample is shown in Fig. 2. According to this, the complete study could be approximated by means of finite difference technique [52]. Because pipes distribution along the absorber plate is considered to be constant, only a portion of the plate was examined. The plate is attached to 15 identical tubes, symmetrically distributed regarding the *y*-axis, thus dividing the plate in 30 similar zones. However, only half of the area between tubes is considered, provided the symmetry in the geometric design. For this reason, only 14 similar zones were considered, as shown in Fig. 2, in

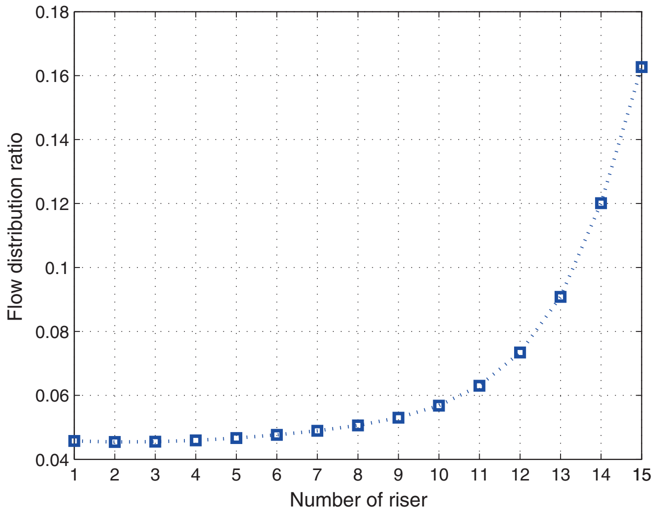


Fig. 3. Flow distribution ratio on each riser.

addition to another two half zones in both plate extremes, regarding x-axis. The boundary line is considered adiabatic, due to the presence of the isolator. Boundary loss is around 3% of the net heat released [49], so it was neglected.

Flow distribution along the risers can be considered constant unless the regime is laminar [22], which happens when the flow rate is very low [46,49]. In this work, Re is smaller than 100 along the circuit of water, due to low flow rate and non-developed flow, making viscous forces more important than inertia ones. Primary hydraulic surface loss in laminar flow can be calculated by the Poiseuille equation, but form loss (secondary loss) analysis needs the application of some experimental coefficients [20]. With the help of these coefficients, pressure loss and flow distribution along the pipes may be analyzed. Another secondary kind of coefficient takes extremely high values, for Re below 100. So, it makes possible to calculate form loss by a general exponential expression depending on Re and the flow ratio in junctions. It derives from the empirical and validated functions observed by Weitbrecht et al. [22].

The Fourier law, related to heat conduction through a material, given by Eq. (1), describes the system dynamics as follows:

$$\alpha\ \Delta T + \frac{\dot{q}_v}{\rho c_p} = \frac{\partial T}{\partial \tau} \Rightarrow \frac{\partial^2 T}{\partial x^2} + \frac{\partial^2 T}{\partial y^2} + \frac{\partial^2 T}{\partial z^2} + \frac{\dot{q}_v}{k_p} = \frac{1}{\alpha}\frac{\partial T}{\partial \tau}$$
$$\text{with}\quad \frac{\alpha}{k_p} = \frac{1}{\rho c_p} \tag{1}$$

where T is the temperature (K), t is the instantaneous time (s), k_p is the conduction coefficient of the absorber (W/(m K)), α is its thermal diffusivity (m^2/s), ρ is its density (kg/m^3), c_p is its specific heat value (J/(kg K)), and $\dot{q}_v$ is the internal heat generation in the absorber (W/m^3).

In fact, the dependent variables presented in Eq. (1) must be optimized by a method that will be explained in detail later. The flow rate differs along each riser, as shown in Fig. 3. The main consequence is the different temperature distribution between the sections of the plate. So, the developed model of heat transfer must be adapted to each riser attached to the flat plate. For this reason, the study is performed in 14 similar portions of pipes of the same geometry (including two half zones in both plate extremes), but with different water flow rate due to hydraulic unbalance caused by the high form loss coefficients associated to the laminar regime.

The complete heat balance considers boundary conditions, that is, the input and output of energy to/from the plate at each time interval and per surface unit (W/m^2). Firstly, the unitary surface heat radiation, q_1'' (W/m^2), is determined from the global incident radiation over the tilted absorber, I_T (W/m^2), reduced by the product transmittance–absorptance of the '$\tau\alpha$' glass-absorber unit, as shown in Eq. (2.a).

$$q_1''(t) = I_T \tau\alpha(t) \tag{2.a}$$

Secondly, the unitary heat loss of the plate, q_2'' (W/m^2), is calculated from the temperature difference between the selected point and the environment, as follows (Eq. (2.b)):

$$q_2''(t) = U_l(t)(T(t) - T_a(t)) \quad \text{with} \quad U_l = U_l\{T(t), T_a(t)\}, \tag{2.b}$$

The global heat loss coefficient, U_l (W/(m^2 K)), is composed of two factors: (a) the loss behind the collector, U_b (W/(m^2 K)), due to the heat conduction through the isolator and the casing, and (b) the convection loss to the atmosphere. Its values depend on the material properties and wind speed. The top loss, U_t (W/(m^2 K)), originates from solar radiation and re-radiation, system tilt, orientation and plate temperature.

Finally, q_3'' (W/m^2) (associated to pipes geometry) provides the available heat that passes through the working fluid, named useful heat. It may be calculated by means of the film coefficient, h [W/(m^2 K)], related to the convection heat transfer from the inner wall of the pipe, with mean temperature T_w (K) and water mean temperature T_f (K), along a differential length Δy (m) in direction y, as shown in Eq. (2.c).

$$q_3''(t) = h(t)(T_w(t) - T_f(t)) = \frac{(\dot{m}_f c_f\ \Delta T_f + \Delta y \pi r_i^2 \rho_f c_f (dT_f/dt))}{(2\pi r_i\ \Delta y)} \tag{2.c}$$

where $\dot{m}_f$ is the fluid flow rate (kg/s), T_o is the room temperature (K), c_f is the water specific heat value (J/(kg K)), ρ_f is the density (kg/m^3), ΔT_f is the increment of temperature (K) and r_i is the internal radius of each riser (m). Finally, this procedure comprises some heat input to the water through the horizontal manifolds before and after the risers. For their determination, Eq. (3) is included. This equation provides the inlet temperature value into each riser.

The very low water flow rate and the small scale provide a non-developed flow into the pipes. Re is small enough to distort the axial speed of the fluid along the riser by buoyancy forces [29]. The filed flow is strongly influenced by Gr and the elevation angle of the riser [30]. It makes impossible to assure the capability of the equations provided by the literature for the determination of the film coefficient, h, only by CFD techniques. Provided the difficulty to carry out an initial approach to achieve an accurate value of h, it is calculated by means of an initial value, h_o, obtained from semi-empirical relations of heat transfer theory and multiplied by a proportionality term associated to the coefficient, k_h, as shown in Eq. (3). To assure coherent results, the optimal value for the coefficient is needed.

$$h(t) = 10^{k_h} h_o(t); \quad h_o = h_o\{k_f, r_i, Nu\} \tag{3}$$

On the other hand, when Biot number, Bi, is evaluated ($Bi = he/k_p$, where e is the thickness of the plate), it gives a value much smaller than one. This means the temperature across the thickness of the plate can be considered constant, giving the same results in both sides of the plate, as found by other researchers [52]. So, the unit plate-pipes can be analyzed as a two-dimension system. According to this, the internal heat generation of Eq. (1) results from the boundary conditions of Eq. (2), adapted to Eq. (4), as follows:

$$\dot{q}_v(t) = \dot{q}_1(t) - \dot{q}_2(t) - \dot{q}_3(t) \text{ in W/m}^3; \quad \dot{q}_1(t) = S = \frac{q_1''(t)}{e};$$
$$\dot{q}_2(t) = \frac{q_2''(t)}{e} \quad \text{and} \quad U_L = \frac{U_l}{e} \tag{4}$$

As can be seen, this simplification leads to the introduction of a volumetric heat transfer loss coefficient, U_L (W/(m^{3}K)), being

necessary to analyze in detail the useful heat. As a result of the proposed two-dimension problem, the temperature of the unit plate-pipes across its section is assumed to be constant. Concerning the risers, this assumption is not accurate because an inner wall temperature for each riser, T_w, is established. This temperature is different from the mean top surface temperature, T_m; temperature set varies from the top to the inner wall. The weld that connects the pipes to the plate is also included in the study. These considerations, besides the geometry and materials of each control volume, difficult the calculation of the global heat transfer coefficient of the plate-fluid, K_C [W/(m^2 K)]. So, the equation of useful heat collected by the working fluid must be recalculated. The simplification from three to two dimensions obliges to accommodate the problem. For this purpose, an equivalent thickness, e_q (m), in addition to a volumetric equivalent heat transfer coefficient, U_c [W/(m^{3}K)], that considers the heat from the top to the inner wall, are evaluated. These terms must include a proportional coefficient depending on the pipe geometry, plate weld and position, called k_{uc}. As happened to k_h term, the optimal value that provides an adequate behavior of the collector depends on time. So the heat released to the fluid matches Eq. (5):

$$\dot{q}'_3(t) = K_c(t)(T_m(t) - T_f(t)) \to \dot{q}_3(t) = \frac{\dot{q}'_3(t)}{e_q};$$
$$e_q = \frac{(e\,\Delta x + \pi(r_e^2 - r_i^2))}{\Delta x}; \quad e = r_e - r_i; \quad K_c(t) = 10^{k_{uc}} \cdot\left(\frac{r_e}{r_i}\cdot\frac{1}{h(t)} + \frac{r_e}{k_p}\ln\left(\frac{r_e}{r_i}\right)\right)^{-1}; \quad \dot{q}_3(t) = U_c(t)(T_m(t) - T_f(t));$$
$$U_C = \frac{K_c(t)}{e_q} = 10^{k_{uc}}\frac{\Delta x}{(e\,\Delta x + \pi(r_e^2 - r_i^2))} \cdot\left(\frac{r_e}{r_i}\cdot\frac{1}{h(t)} + \frac{r_e}{k_p}\ln\left(\frac{r_e}{r_i}\right)\right)^{-1} \tag{5}$$

Eqs. (4) and (5) help to determine the temperature in particular points of the plate. The one dimensional useful heat that passes to the water, $q_{u'}(t)$ (W/m), considering steady state conditions and Δy, may be calculated according to Eq. (6) as follows:

$$q'_u(t)\big|_{\Delta y} = \frac{\dot{m}_f c_f\,\Delta T_f}{\Delta y} = 2\pi r_i h(t)(T_w - T_f) \tag{6}$$

2.2.1. Steady state equations

For each (*i*,*j*) point of the mesh, and depending on the increments Δx and Δy on the absorber fin, the numeric adaptation of the set of Eqs. (1)–(6) for steady state analysis follows the expressions:

$$\text{general form}: T_{i-1,j} + T_{i+1,j} + T_{i,j-1} + T_{i,j+1} - T_{i,j}\left[4 + \frac{U_L}{k_p}\Delta x\ \Delta y\right] = -\frac{\Delta x\,\Delta y}{k_p}(S + U_L T_o)$$

$$\text{adiabatic riser boundary form}: 2T_{i-1,j} + T_{i,j-1} + T_{i,j+1} - T_{i,j}\left[4 + \frac{U_L + U_c}{k_p}\Delta x\ \Delta y\right] + T_{i+1,j}\frac{U_c}{k_p}\Delta x\,\Delta y = -\frac{\Delta x\,\Delta y}{k_p}(S + U_L T_o) \tag{7.a}$$

$$\text{adiabatic fin boundary form}: 2T_{i+1,j} + T_{i,j-1} + T_{i,j+1} - T_{i,j}\left[4 + \frac{U_L}{k_p}\Delta x\ \Delta y\right] = -\frac{\Delta x\,\Delta y}{k_p}(S + U_L T_o)$$

For a finite different approach, *m* corresponds to the number of nodes in '*x*' direction (*i* varies from 1 to *m*). Moreover, the working fluid receives a certain quantity of heat when passing from *y* = *j* to *j* + *1*. It flows into the riser placed at each extreme of the mesh, as shown in Fig. 2. Thus, an additional equation for each one, i.e. Eq. (6), is needed. A numerical approach is presented in Eq. (7.b), considering both limits ($T_{0,j}$ and T_{m+1} correspond to fluid temperatures associated to nodes *r* = 1 and *r* = *m*, respectively).

$$T_{1,j}\Gamma + T_{0,j-1} - T_{0,j}(1+\Gamma) = 0; \qquad T_{m,j}\Gamma + T_{m+1,j-1} - T_{m-1,j}(1+\Gamma') = 0; \qquad \Gamma = \frac{2\pi r_i\,\Delta y h}{2\dot{m}_{f,r} c_f}; \tag{7.b}$$

The set of $(m+2)n$ Eqs. (7.a) and (7.b) is used to establish the basic model in the plate-pipes unit, considering the unknown temperatures on the plate (two-dimension) and the working fluid passing through the tube (one-dimension). This is referred to the system portion described above (Fig. 2).

A non-linear set of equations that must be solved by iteration is presented. For this purpose, plate temperature is considered to be room temperature. Then, the rest of the parameters such as U_L, U_c, *h* and *S* will be calculated. A matrix calculus is built-up, resulting in a new set of plate temperatures. This process continues until temperatures converge to constant values. It is very important to advise that this iterative process belongs to the optimization process explained below, considering known all the parameters that define $\overline{UP}^n$.

To evaluate the set of Eq. (7) for each riser, the inlet water temperature must be estimated. For this purpose, a light modification is adopted and applied to the input horizontal manifold. In this pipe, the temperature is evaluated for only one dimension (*x*-axis), between the junctions that connect two consecutive risers. Provided that the global input flow temperature and flow distribution throughout the unit are known, the equations set can be successfully solved. It gives information about the heat delivered to the water in the lower pipe (with inner radius r'_i), from the riser *p* to the riser *p* + 1, separated Δl. It results in the following expression:

$$T_{p-1} + T_{p+1} - T_p\left[2 + \frac{U_L + U_c}{k_p}\Delta x'\ \Delta y'\right] + T_{f,p}\frac{U_c}{k_p}\Delta x'\ \Delta y' = -\frac{\Delta x'\ \Delta y'}{k_p}(S + U_L T_o) \tag{8.a}$$

$$T_{f,p}\Gamma' + T_{f,p-1} - T_{f,p+1}(1+\Gamma') = 0; \quad \Gamma' = \frac{2\pi r'_i\,\Delta l h}{2\dot{m}'_f c_f}; \tag{8.b}$$

where $\Delta x' = \Delta l$, $\Delta y' = 2r'_i$. The fluid that flows through the lower pipe is non-uniform and continuously reduced, as shown in Fig. 3. Once the evaluation of Eq. (7) is finished, the upper pipe is analyzed. This will provide the outlet global temperature of the fluid.

The proposed numerical analysis has been compared to other analytical methods from the literature, providing similar results for the film coefficient *h* and same qualitative tendencies for pressure loss [53].

2.2.2. Transient state equations

When Eqs. (7.a), (7.b), (8.a) and (8.b) are used under transient state condition, the inclusion of settings that consider the derivative of temperature *vs.* time is required. To evaluate it, an implicit

method has been proposed. The method is very stable and does not require extremely narrow intervals of time. In this case, a similar equations set depending on known values of characteristics and temperatures of a previous state, k, is introduced [52]. Once temperatures are known for $t = k$, they will be calculated for $t = k + 1$ using an additional coefficient. The general coefficients from Eqs. (7.a) and (7.b) are changed according to Eqs. (9.a) and (9.b), respectively (other terms and equations are adapted accordingly).

$$T_{i-1,j}^{k+1} + T_{i+1,j}^{k+1} + T_{i,j-1}^{k+1} + T_{i,j+1}^{k+1} - T_{i,j}^{k+1}A = -\frac{\Delta x\,\Delta y}{k_p}(S + U_L T_o) - rT_{i,j}^{k};$$
$$A = \left[4 + \frac{U_L}{k_p}\Delta x\,\Delta y + r\right];\ r = \frac{\Delta x\,\Delta y}{\alpha\,\Delta t} \tag{9.a}$$

$$T_{i,j}^{k+1}\Gamma + T_{i\pm1,j-1}^{k+1} - T_{i\pm1,j}^{k+1}(1 + \Gamma + \Gamma_p)$$
$$= -\Gamma_p T_{i\pm1,j}^{k} \quad \Gamma_p = \frac{\pi r_i^2\,\Delta y\,\rho_f}{4\dot{m}_f\,\Delta t};\quad \text{for } i = 1 \text{ and } i = m \tag{9.b}$$

2.3. Solution to model optimization procedure

The proposed procedure consists in the following steps:

a) The system and its model are defined analytically and numerically for one and two dimensions [46,54]. Initially, the values of certain physical properties of the collector materials (input parameters of the model) are provided according to the literature. These parameters are integrated into the vector of characteristics $\overline{UP}$ that may vary for each instant of time n (named $\overline{UP}^n$). Initially, the parameters included in this vector are the following:
- k_e: extinction coefficient of the covering glass (m^{-1})
- n_2: refraction index of the glass
- α_θ: directional absorbance of the copper black plate, considering an incident angle of irradiation over the tilted surface, θ, depending on tilt, latitude, declination, solar time, etc.
- ε_p: plate emissivity
- ε_g: glass emissivity
- k_{iT}: conduction heat transfer coefficient of insulation [W/(mK)]
- k_p: conduction heat transfer coefficient of copper [W/(mK)]
- k_h: proportionality parameter associated to the tube inner wall film coefficient (convection heat transfer), h_o [W/(m^2 K)] [46].
- k_q: proportionality parameter associated to the volumetric equivalent heat transfer coefficient, U_C [W/(m^3 K)], considering two-dimensional systems [46].

b) Once the system is defined, operating conditions are tested two hours a day. These conditions include different days and collector tilts. For each instant of time 'n', the vector $\overline{SP}^n$ contains the following input variables associated to both the irradiation and the system behavior (i.e. flow rate and temperatures):
- $\dot{m}_f$: water flow rate (kg/s)
- s: collector tilt (rad)
- φ: latitude (rad)
- ω: timing angle (rad)
- δ: declination (rad)
- γ: azimutal angle (rad)
- θ: incident angle of beam irradiance over the tilted surface (rad)
- I_T: global irradiance over the tilted collector (W/m^2).
- T_a: room temperature (K)
- T_{fi}: fluid inlet temperature (K)

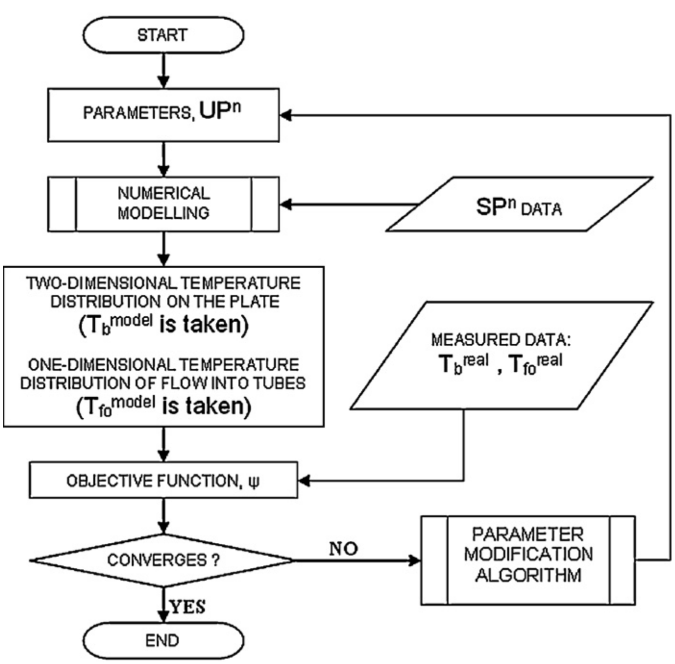


Fig. 4. Flow chart of the identification process (steps a–c).

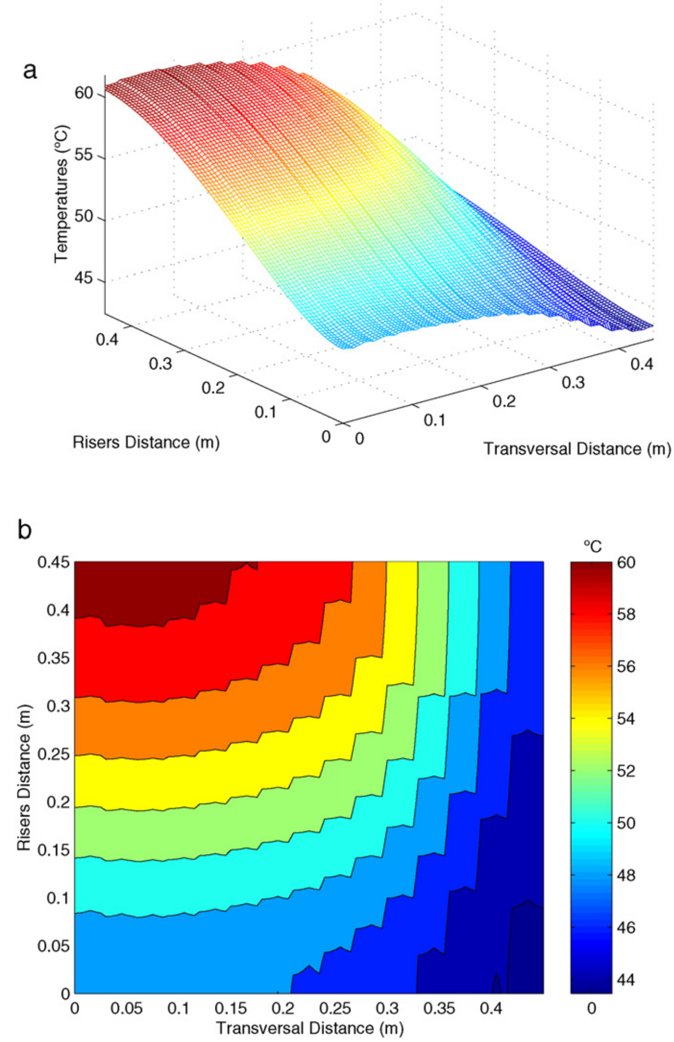


Fig. 5. Temperature distribution on the absorber: (a) isometric view; (b) plant view.

Table 2
Characteristic angles of the collector for some random measures.

Stationary test no.	Collector tilt s (°)	Latitude φ (°)	Solar hour angle ω (°)	Declination δ (°)	Azimutal angle γ (°)	Incident angle of direct irradiation θ (°)
1	38	38	15	20.73	0	25.56
2	28	38	22.5	21.27	0	24.47
3	48	38	15	21.43	0	34.9

Table 3
Input–output data values of random measures from Table 2.

Stationary test no.	Solar incident radiation I_T (W/m^2)	Room temperature T_o (°C)	Inlet water temperature T_i (°C)	Outlet water temperature T_o (°C)	Bulb plate temperature T_p (°C)	Fluid flow rate $\dot{m}_f$ (kg/h)
1	936.8	23.2	31	50.5	57	6.42
2	900.8	19.4	26	39	49.5	7.35
3	862.1	25.3	33	46	50.5	7.35

Table 4
Optimized values for unknown parameters after the identification process shown in Tables 2 and 3.

Test no.	k_e (mm^{-1})	n_2	α_θ	ε_p	ε_g	k_{It} (W/(m K))	k_p (W/(m K))	U_c (W/(m^3 K))	h (W/(m^2 K))
Initial	0.4	1.526	0.801	0.039	0.88	0.029	402.4	11.8×10^3 Initial value for test No. 1	11 Initial value for test No. 1
1	0.4022	1.5649	0.7543	0.0391	0.8804	0.0293	457.7	11.9×10^4	58.84
2	0.4016	1.5667	0.7405	0.0391	0.8802	0.0292	423.71	9.1×10^4	35.7
3	0.4019	1.5569	0.7668	0.0391	0.8803	0.0293	474.38	18.4×10^4	69

c) To undertake the simulation, the variation of the input data of the vector $\overline{SP}^n$ *vs.* time is required. On the other hand, vector $\overline{UP}^n$, built-up with the previously mentioned unknown terms (provided by the literature), could lead to a weak approximation to reality. Thus, the target of the application at this step is to identify the real values of those unknown terms, simulating the real behavior of the collector over the time. This method is used for steady state analysis. The objective function Ψ is calculated from the sum of squares of differences between the model response and the empirical system response values, associated to both the outlet temperature of the working fluid from the collector T_{fo} (K) and the plate temperature of a representative point of the plate, T_b (K), placed near to the top of the absorber (the real value is measured by a bulb thermometer), as shown in Figures 1 and 2. So, the objective function remains as follows:

$$\Psi = (T_{fo}^{\text{real}} - T_{fo}^{\text{model}})^2 + (T_b^{\text{real}} - T_b^{\text{model}})^2 \quad (10)$$

If hydraulic friction loss and fluid flow rate distribution are considered, then the objective function must incorporate quadratic terms related to pressure in some points of the circuit. This additional approach has been previously evaluated in the same system but working as a thermosyphon, providing accurate results [53]. The identification procedure is applied n times to determine the parameters values of $\overline{UP}^n$, thus minimizing the described function Ψ. The identification process described in this step has been summarized in Fig. 4.

d) Next step comprises the determination of $\overline{SP}^n$ components (i.e. heat release by incident radiation and angles related to solar

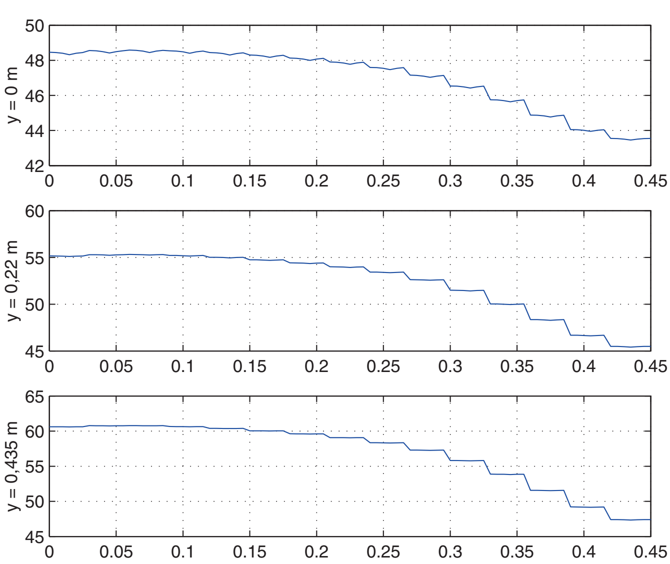


Fig. 6. Temperature variation (°C) in three cross sections of the absorber, transversally to fluid movement at different locations of the flat plate.

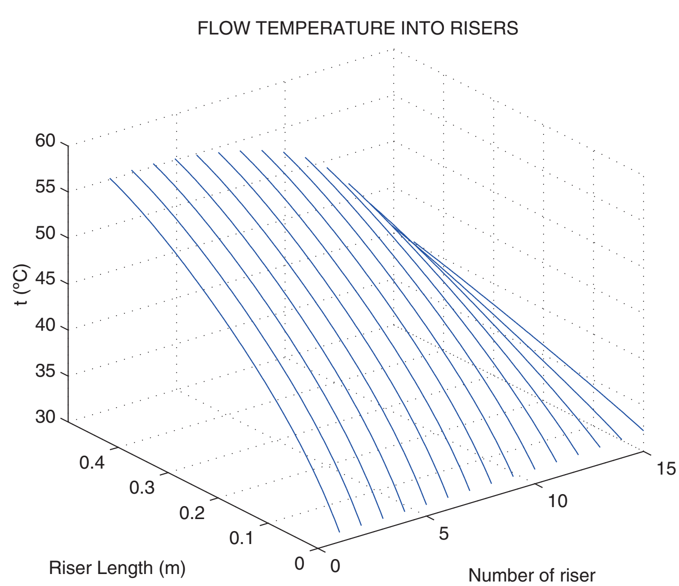


Fig. 7. Water temperature evolution through pipes.

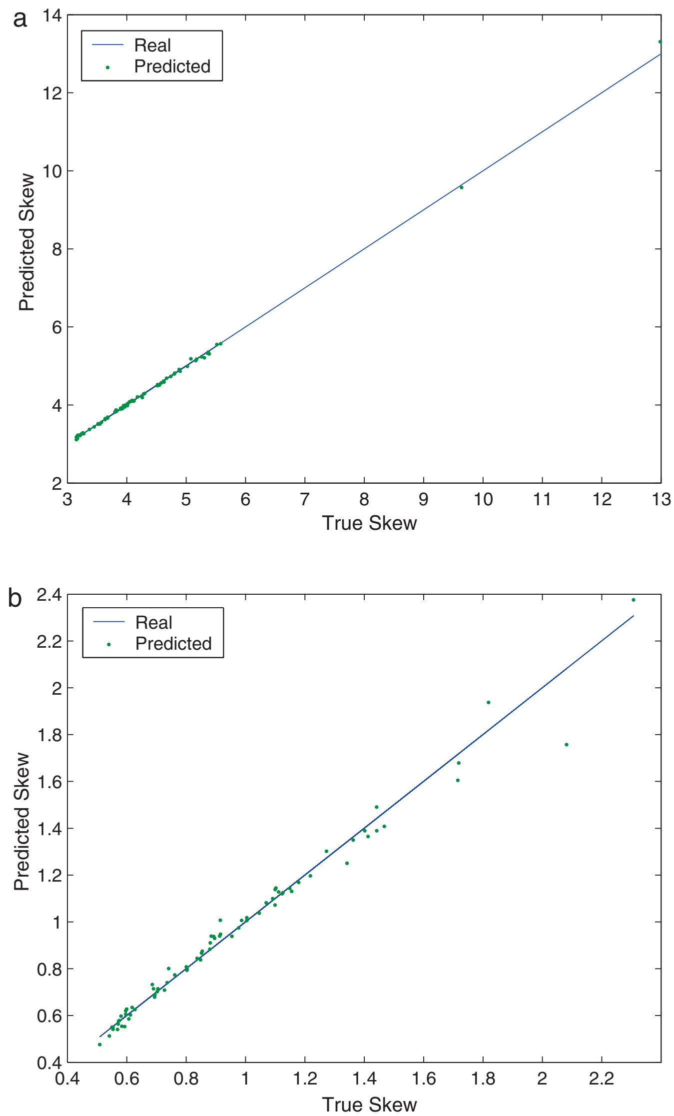


Fig. 8. Comparison between real and predicted values for parameters k_{uc} (a) and Nu (b).

time) and the system response data (i.e. plate temperatures) that fit the real values of the parameters belonging to $\overline{UP}^n$. If the previous expressions do not suffice to approximate the desired functions, other kind of equations must be taken into consideration, i.e. a multivariate analysis depending on the operating variables included in $\overline{SP}^n$ [55]. Statistical fitting functions for these parameters must be analyzed. These functions depend on the operating parameters included in the $\overline{SP}^n$ vector, making them time independent. Finally, the initial model must be redefined.

e) Once the model is redefined, the transient state model is checked for each complete daily test.

3. Results

This section includes validation of the numerical model, parameters identification procedure and transient regime evaluations. Separation between nodes in each of the 14 mentioned regions is calculated considering $\Delta x = \Delta y = 0.005$ m, resulting in $m = 7$. This means there are 637 nodes (7×91) over each absorber fin (Fig. 2). In the plate extremes, only one riser and half absorber fin are

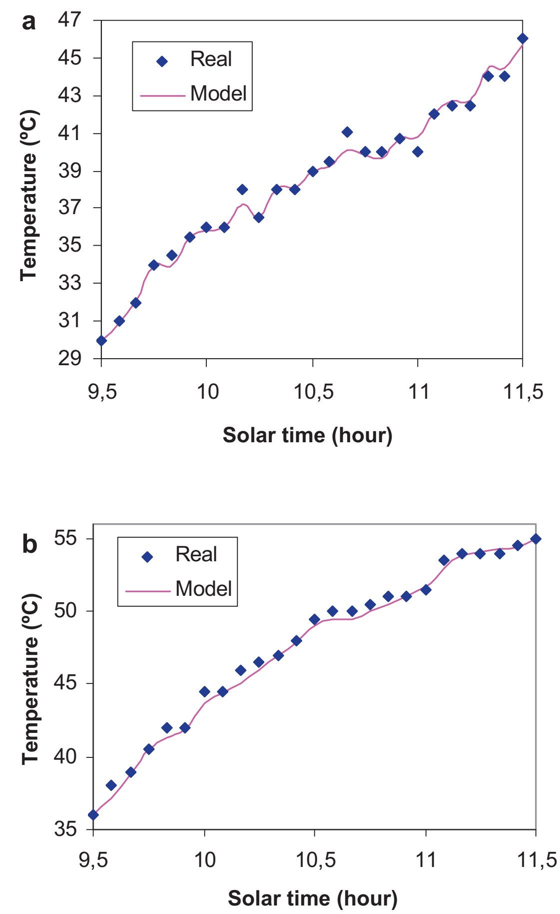


Fig. 9. Experimental and modelled results at 28° tilt: (a) water outlet temperature evolution; (b) absorber plate temperature evolution.

considered. So, the number of nodes is 364 (4×91). Also, the fluid temperatures in the boundary limits, considering the x-axis, have been considered. Thus, the set of equations is composed of 810 equations, with 810 unknown values of temperatures linked to each analyzed absorber portion. The intermediate space between nodes in the upper and lower tubes is 0.03 m.

3.1. Steady state parameter identification

Initially, the unknown vector is defined with data from the literature. Parameters identification process of $\overline{UP}^n$ is carried out randomly over the time. Data belonging to vectors $\overline{SP}^n$ are depicted in Tables 2 and 3, while Table 4 shows the optimization results of $\overline{UP}^n$ under the same conditions.

Fig. 5 shows the temperatures distribution over the plate in a particular case study, while Fig. 6 exhibits three different transversal sections. In agreement with the literature, the variation is small, but increases with the distance from the riser [17]. The bulb thermometer shows same values for modelled and real temperatures. Also, extreme values of input and output water temperatures match real ones. Fig. 7 depicts one-dimensional temperature variation of the fluid flow into each riser.

As a result of the first evaluation, it can be seen that material properties show values close to those initially estimated. Variations in the glass covering, isolation and copper plate properties demonstrate that values from the literature are appropriate to the simulation process [54]. In fact, they almost satisfy the condition of monotonicity needed to assure an unique solution of the IHTP [40]. For this reason, these values are considered known and removed

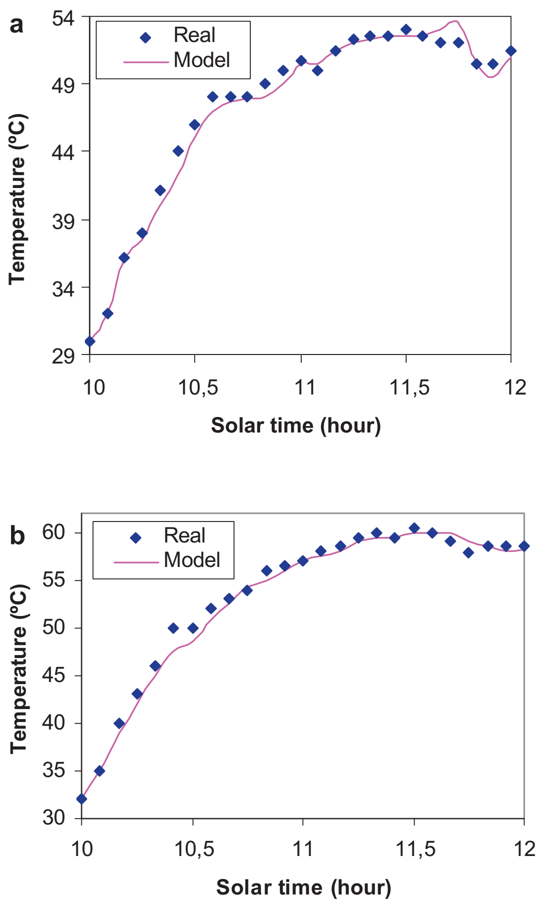


Fig. 10. Experimental and modelled results at 38° tilt: (a) water outlet temperature evolution; (b) absorber plate temperature evolution.

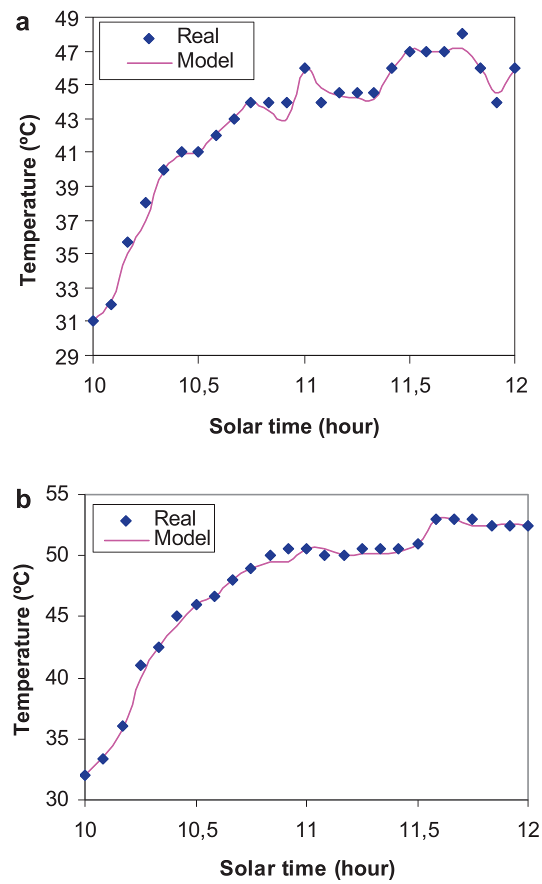


Fig. 11. Experimental and modelled results at 48° tilt: (a) water outlet temperature evolution; (b) absorber plate temperature evolution.

from the vector of unknown parameters $\overline{UP}^n$. Thus, computational charge can be reduced significantly in the next step. On the other hand, parameters associated to heat transfer experiment important variations compared to the initial estimation (from 5 to 10 times the original value) provided by Eqs. (3) and (5) due to model simplifications. The same conclusion can be drawn when analytical functions are applied [49]. Only two terms belonging to $\overline{UP}^n$, namely k_{uc} and k_h, vary Uc and h values, respectively, over the time. Flow regime with a very low Re makes difficult to calculate the flow rate into each riser, the heat transfer mechanism and the real convection coefficient. This model assumes a two-dimension problem, considering the pipes as flat surfaces. An accurate study of the associated terms Uc and h, considering physical and geometric properties, is required.

Next step consists in the identification of the data collected two hours per day, during several days. As mentioned above, only the parameters k_{uc} and k_h belong to the vector $\overline{UP}^n$ and will be optimized. Also, there is a relation between U_c and h, as shown in Eq. (5).

3.2. New functions and model review

Once the selected parameters are identified, a relation between U_c and temperature is observed. So, next step requires to find out a regression function for parameter k_{uc}, providing the equivalent heat transfer coefficient, U_c. With the help of a multivariate analysis, the parameter is adjusted by an exponential/potential function, f_1 [55].

To approximate each parameter (output variable), regression functions with exponential/potential shape, f_l, are required. For each output function, f_l, it can be found wl different input variables, X_{ul}, conforming the vector $\overline{SP}^n$. The function is as follows:

$$f_l = a_l X_{1l}^{b_{1l}} X_{2l}^{b_{2l}} \ldots X_{wl}^{b_{wl}}; \quad \forall u \in (1, w) \to X_{ul} \in \bar{s} \tag{11}$$

where a_j and b_{ul} are constants of the function when it is successfully developed.

Initially, it is assumed that f_1 depends on different temperatures, namely inlet and outlet fluid, room and plate temperatures. Nevertheless, this first approach is not enough to ensure a good fitting. So, other parameter like solar irradiation over the tilted surface is needed. According to this, the best result for f_1 [showing a standard deviation of 0.033 of the root mean square (RMS) error applied to the function] is found when the released solar heat under different temperatures is taken into consideration, as shown in Eq. (12) (where a_1 is constant).

$$k_{uc} = f_1(a_1, T_p, T_{fi}, T_{fo}, T_o, I_t) \tag{12}$$

In relation with the film coefficient, h, it can be seen that final data present a great dispersion. This confirms the necessity of establishing a new function to approximate Nu and identify the real film coefficient h over the time. It shows there is a non-developed fluid flowing along the risers, even presenting internal recirculation, as indicated by Zghal [29]. So, a deep analysis of the involved processes, aided by CFD techniques, is required. However, this situation goes beyond the objectives of this article. So, a regression function to estimate h and k_{uc} is enough for the proposed study.

In the present work, k_h helps to determine the real value of h and subsequently Nu. Then, the procedure for searching an

approximation function f_2 by stochastic methods is repeated and *Nu* is calculated by the input variables X_{u2}. Between these variables, the non-dimensional parameters *Re*, *Pr* and *Gr* provide important information about water flowing into the risers and inner wall temperatures. Nevertheless, the simplification and the non-developed fluid flow could lead to misstatements during heat transmission modelling. So, the inclusion of other parameters is required. As a result, the adequate function includes the input parameters shown in Eq. (13) (where a_2 is constant), besides irradiation and tilt. This last term affects the heat distribution and the transversal velocity of the fluid flow. So, determination of *h* into the risers can be easily undertaken using expression (13), as follows:

$$h = \frac{Nu\, k_f}{2R_i}; \quad Nu = f_2(a_2, Re, Pr, Gr, T_p, T_{fi}, T_{fo}, T_o, I_t, \theta); \qquad (13)$$

Results show a standard deviation of the RMS error of 0.11. Fig. 8 depicts the correlation between the functions f_1 and f_2. Standard deviations are very low, thus indicating results are in agreement with parameters values from Eqs. (12) and (13).

Approaches provided by Eqs. (12) and (13) allow the validation of the proposed numerical model with available data. Nevertheless, more general and useful correlations should be considered in future works, thus extending the experiments to fluid flows, temperatures and friction losses data [24,25,28,50,51]. In this sense, increasing the number of sensors is crucial. Also, to improve the model, Eq. (3) must be substituted by Eq. (13), while k_{uc} must be determined using Eq. (12) and applied to Eq. (5).

3.3. Transient state analyses further to model review. Final validations

Once the model has been revised, the transient state is analyzed. Considering the input data, distributions are in agreement with real data, as shown in Figs. 5–7, but depending on both time and previous state. From these distributions, two data are selected and compared with real values: outlet water temperature and bulb temperature (located on the plate). Some results are shown in Figs. 9–11.

Approaches present good accuracy. Although certain delays are observed, they are caused by the time interval. This problem can be fixed by increasing the computing time, but it does not guarantee better approximations. In any case, the previous model, in addition to new approximation functions ensures enough accuracy to simulate the real behavior of this particular system.

Similar results are found by other researchers, considering the transient behavior of the collector [35], as shown in Figs. 9–11. Although results validate the proposed model, a deeper study of the thermo-hydraulic mechanisms may be considered in future works. Nevertheless, it is important to notice that the target of this study was to estimate the temperature distribution over the plate and into de pipes, and this objective has been successfully reached.

4. Conclusions

A general strategy that helps to validate a solar collector model where some parameters are difficult to determine, under both non-steady and non-uniform states, has been proposed. In this case, the specific conditions of the fluid regime and the geometry of the collector make difficult to understand the dynamic behavior of the system. To avoid the use of complex numerical techniques, such as CFD or finite element method (FEM), a highly accurate model including simplifications of the physical unit (plate-pipes) has been developed. As an advantage, this process only requires a few sensors. For this reason, it makes possible the analyses in equipments without many sophisticated sensors (as used in heat-pipes studies). Temperatures distribution of both absorber and water gives qualitatively similar results to previous works found in the literature. Moreover, both steady and transient regimes can be validated with experimental results, thus demonstrating the accuracy of the model. Results also show that materials properties are in close agreement with the values given by the literature. This means low uncertainties if similar values are used, thus avoiding the need of highly accurate initial data.

Apart from the type of model, both the identification process and the approximation functions constitute two fundamental steps. Nevertheless, the processes depend on the following conditions:

1. The identification process is based on a non-linear optimization procedure over a quadratic continuous function that is a derivative dependent function. In case the objective function exhibits a high discontinuity, the proposed methodology could be ineffective. If so, to optimize the function, other techniques such as Genetic Algorithms must be evaluated.
2. Considering parameters approximation functions, exponential regression functions have been developed by multivariate analysis of variance. However, other functions may also be evaluated, i.e. linear functions and potential functions. Including some modifications to the exponential regression functions provides another possibility to take into consideration. In this case, stochastic models cannot be used. So, the aid of CFD techniques is recommended.

The proposed methodology allows the analysis of the system under a huge range of different conditions, such as materials and geometry changes. Also, it makes possible to find out the optimum value of the pipes diameter and the distance between them to maximize the captured energy, among many other possibilities. A further analysis to optimize the geometry and dimensions may be developed. In this sense, a future target could be to modify them to maximize the collection of energy, as mentioned in the introduction of this paper.

References

[1] Hernandez-Escobedo Q, Manzano-Agugliaro F, Zapata-Sierra A. The wind power of Mexico. Renewable & Sustainable Energy Reviews 2010;14:2830–40.
[2] Manzano-Agugliaro F, Escobedo QCH, Sierra AJZ. Use of bovine manure for ex situ bioremediation of diesel contaminated soils in Mexico. Itea-Informacion Tecnica Economica Agraria 2010;106:197–207.
[3] Hernandez-Escobedo Q, Manzano-Agugliaro F, Gazquez-Parra JA, Zapata-Sierra A. Is the wind a periodical phenomenon? The case of Mexico. Renewable & Sustainable Energy Reviews 2011;15:721–8.
[4] Banos R, Manzano-Agugliaro F, Montoya FG, Gil C, Alcayde A, Gomez J. Optimization methods applied to renewable and sustainable energy: a review. Renewable & Sustainable Energy Reviews 2011;15:1753–66.
[5] Ssen Z. Solar energy in progress and future research trends. Progress in Energy and Combustion Science 2004;30:367–416.
[6] Dagdougui H, Ouammi A, Robba M, Sacile R. Thermal analysis and performance optimization of a solar water heater flat plate collector: Application to Tetouan (Morocco). Renewable & Sustainable Energy Reviews 2011;15:630–8.
[7] Pillai IR, Banerjee R. Methodology for estimation of potential for solar water heating in a target area. Solar Energy 2007;81:162–72.
[8] Tchinda R. A review of the mathematical models for predicting solar air heaters systems. Renewable & Sustainable Energy Reviews 2009;13:1734–59.
[9] Hellstrom B, Adsten M, Nostell P, Karlsson B, Wackelgard E. The impact of optical and thermal properties on the performance of flat plate solar collectors. Renewable Energy 2003;28:331–44.
[10] Kundu B. Performance analysis and optimization of absorber plates of different geometry for a flat-plate solar collector: a comparative study. Applied Thermal Engineering 2002;22:999–1012.
[11] Luminosu I, Fara L. Determination of the optimal operation mode of a flat solar collector by exergetic analysis and numerical simulation. Energy 2005;30:731–47.
[12] Torres-Reyes E, Navarrete-Gonzalez JJ, Zaleta-Aguilar A, Cervantes-de Gortari JG. Optimal process of solar to thermal energy conversion and design of irreversible flat-plate solar collectors. Energy 2003;28:99–113.
[13] Shariah AM, Rousan A, Rousan KK, Ahmad AA. Effect of thermal conductivity of absorber plate on the performance of a solar water heater. Applied Thermal Engineering 1999;19:733–41.
[14] Hussein HMS, Mohamad MA, El-Asfouri AS. Optimization of a wickless heat pipe flat plate solar collector. Energy Conversion and Management 1999;40:1949–61.

[15] Badescu V. Optimum fin geometry in flat plate solar collector systems. Energy Conversion and Management 2006;47:2397–413.
[16] Lates R, Visa I, Lapusan C. Mathematical optimization of solar thermal collectors efficiency function using MATLAB. Athens: World Scientific and Engineering Acad and Soc; 2008.
[17] Duffie JA, Beckman WA. Solar engineering of thermal processes. 3rd ed. New York: John Wiley & Sons Inc.; 2006.
[18] Reddy KS, Avanti P, Kaushika ND. Finite time thermal analysis of ground integrated-collector-storage solar water heater with transparent insulation cover. International Journal of Energy Research 1999;23:925–40.
[19] Saldana JGB, Diez PQ. Experimental–computational evaluation of a solar water heating system. Leiden: A a Balkema Publishers; 2004.
[20] Streeter V, Wylie BE, Bedford KW. Fluid mechanics. 9th ed. New York: McGraw-Hill; 1998.
[21] Sumathy K, Venkatesh A, Sriramulu V. Heat-transfer analysis of a flat-plate collector in a solar thermal pump. Energy 1994;19:983–91.
[22] Weitbrecht V, Lehmann D, Richter A. Flow distribution in solar collectors with laminar flow conditions. Solar Energy 2002;73:433–41.
[23] Kumar A, Prasad BN. Investigation of twisted tape inserted solar water heaters—heat transfer, friction factor and thermal performance results. Renewable Energy 2000;19:379–98.
[24] Baker LH. Film heat-transfer coefficients in solar collector tubes at low Reynolds numbers. Solar Energy 1967;11:78–84.
[25] Oliver DR. The effect of natural convection on viscous-flow heat transfer in horizontal tubes. Chemical Engineering Science 1962;17:335–50.
[26] Li XL, You SJ, Zhang H, You ZP. Thermal performance of solar air collector with slit-like perforations. Journal of Central South University of Technology 2009;16:145–9.
[27] Papanicolaou E. Transient natural convection in a cylindrical enclosure at high Rayleigh numbers. International Journal of Heat and Mass Transfer 2002;45:1425–44.
[28] Wang AB, Travncek Z. On the linear heat transfer correlation of a heated circular cylinder in laminar crossflow using a new representative temperature concept. International Journal of Heat and Mass Transfer 2001;44:4635–47.
[29] Zghal M, Galanis N, Nguyen CT. Developing mixed convection with aiding buoyancy in vertical tubes: a numerical investigation of different flow regimes. International Journal of Thermal Sciences 2001;40:816–24.
[30] Orfi J, Galanis N. Developing laminar mixed convection with heat and mass transfer in horizontal and vertical tubes. International Journal of Thermal Sciences 2002;41:319–31.
[31] Dahl SD, Davidson JH. Performance and modeling of thermosyphon heat exchangers for solar water heaters. Journal of Solar Energy Engineering Trans-ASME 1997;119:193–200.
[32] Belessiotis V, Mathioulakis E. Analytical approach of thermosyphon solar domestic hot water system performance. Solar Energy 2002;72:307–15.
[33] Hilmer F, Vajen K, Ratka A, Ackermann H, Fuhs W, Melsheimer O. Numerical solution and validation of a dynamic model of solar collectors working with varying fluid flow rate. Solar Energy 1999;65:305–21.
[34] Oliva A, Costa M, Segarra CDP. Numerical simulation of solar collectors—the effect of nonuniform and nonsteady state of the boundary-conditions. Solar Energy 1991;47:359–73.
[35] Prapas DE, Norton B, Milonidis E, Probert SD. Response functions for solar-energy collectors. Solar Energy 1988;40:371–83.
[36] Kazeminejad H. Numerical analysis of two dimensional parallel flow flat-plate solar collector. Renewable Energy 2002;26:309–23.
[37] Cerne B, Medved S. Determination of transient two-dimensional heat transfer in ventilated lightweight low sloped roof using Fourier series. Building and Environment 2007;42:2279–88.
[38] Chuawittayawuth K, Kumar S. Experimental investigation of temperature and flow distribution in a thermosyphon solar water heating system. Renewable Energy 2002;26:431–48.
[39] Hermann M. FracTherm—fractal hydraulic structures for energy efficient solar absorbers and other heat exchangers. In: Proc of Eurosun 2004. 2004.
[40] Moultanovsky AV, Rekada M. Inverse heat conduction problem approach to identify the thermal characteristics of super-hard synthetic materials. Inverse Problems in Engineering 2002;10:19–39.
[41] Baccoli R, Ubaldo C, Mariotti S, Innamorati R, Solinas E, Mura P. Graybox and adaptative dynamic neural network identification models to infer the steady state efficiency of solar thermal collectors starting from the transient condition. Solar Energy 2010;84:1027–46.
[42] Wu SK, Chu HS. Inverse determination of surface temperature in thin-film/substrate systems with interface thermal resistance. International Journal of Heat and Mass Transfer 2004;47:3507–15.
[43] Gill PE, Murray W, Wright MH. Practical optimization. 11th edition ed. London: Academic Press; 1997.
[44] Amer EH, Nayak JK, Sharma GK. A new dynamic method for testing solar flat-plate collectors under variable weather. Energy Conversion and Management 1999;40:803–23.
[45] Engl HW, Fusek P, Pereverzev SV. Natural linearization for the identification of nonlinear heat transfer laws. Journal of Inverse and III-posed Problems 2005;13:567–82.
[46] Cruz-Peragon F, Dorado MP, Montoro V, Palomar JM, Garcia AI. Pequeño sistema térmico de captación solar para prácticas de laboratorio. In: Proc of III Jornadas nacionales de Ingeniería Termodinámica. 2003.
[47] Norton B, Eames PC, Lo SNG. Alternative approaches to thermosyphon solar-energy water heater performance analysis and characterisation. Renewable & Sustainable Energy Reviews 2001;5:79–96.
[48] Allen MB, Isaacson EL. Numerical analysis for applied science. New York: John Wiley and Sons; 1998.
[49] Cruz-Peragon F. Análisis de metodologías de optimización inteligentes para la determinación de la presión en cámara de combustión para motores alternativos de combustión interna por métodos no intrusivos. Seville: University of Seville, Spain; 2005.
[50] Incropera FP, DeWitt DP, Bergman TL, Lavine AS. Fundamentals of heat and mass transfer. 6th ed. New York: John Wiley & Sons Inc.; 2006.
[51] Barletta A, di Schio ER. Effect of viscous dissipation on mixed convection heat transfer in a vertical tube with uniform wall heat flux. Heat and Mass Transfer 2001;38:129–40.
[52] Ketkar SP. Numerical thermal analysis. New York: American Society of Mechanical Engineers; 1999.
[53] Cruz-Peragón F, Montoro V, Palomar JM, Dorado MP. Identificación de parámetros críticos en el comportamiento de un sistema térmico solar por termosifón. In: Proc of IV Jornadas nacionales de ingeniería termodinámica. 2005.
[54] Cruz-Peragón F, Dorado M, Palomar J, Montoro V. Parameter identification for determining one and two-dimensional temperature distribution in a flat plate solar collector. Germany, Freiburg: Eurosun; 2004.
[55] Canavos GC. Applied probability and statistical methods. New York: McGraw-Hill; 1984.